A solar optical hyperspectral library of rare earth-bearing minerals, rare earth oxides, copper-bearing minerals and Apliki mine surface samples

5   Friederike Koerting[1], Nicole Koellner[1], Agnieszka Kuras[1], Nina K. Boesche[1], Christian Rogass[1], Christian Mielke[1], Kirsten Elger[1], Uwe Altenberger[2]

[1] GFZ German Research Centre for Geosciences, Potsdam, 14473, Germany
[2] University of Potsdam, Institute of Geosciences, Potsdam, 14476, Germany

Correspondence to: Friederike Koerting (koerting@gfz-potsdam.de)

Abstract. Mineral resource exploration and mining is an essential part of today's high-tech industry. Elements such as rare
15   earth elements (REE) and copper are, therefore, in high demand. Modern exploration techniques from multiple platforms
(e.g. space- and airborne), to detect and map the spectral characteristics of the materials of interest, require spectral libraries
as an essential reference. They include field and laboratory spectral information in combination with geochemical analyses
for validation. Here, we present an extensive collection of REE- and copper-related hyperspectral spectra with associated
geochemical information. The libraries contain spectra from rare earth element oxides, REE-bearing minerals, copper-
20   bearing minerals and mine surface samples from the Apliki copper-gold-pyrite-mine in the Republic of Cyprus. The samples
were measured with the HySpex imaging spectrometers in the visible near infra-red (VNIR) and short wave infra-red
(SWIR) range (400 – 2500 nm). The geochemical validation of each sample is provided with the spectra. The spectral library
is openly available to assist future mineral mapping campaigns and laboratory spectroscopic analyses. The spectral libraries
and corresponding geochemistry are published via GFZ Data Services with the following DOIs:
25   http://doi.org/10.5880/GFZ.1.4.2019.004 (REE elements, Koerting et al., 2019a), http://doi.org/10.5880/GFZ.1.4.2019.003
(Copper bearing minerals. Koellner et al., 2019), and http://doi.org/10.5880/GFZ.1.4.2019.005 (copper bearing minerals
from the Apliki copper-gold-pyrite mine in Cyprus, Koerting et al., 2019b).

30

1. Introduction

Reflectance spectroscopy is based on measuring the reflected solar radiation from a material of interest. It uses photosensitive detectors to record and analyse light reflected or scattered from the surface. The reflected light is unique for each material and acts like a spectral "fingerprint". Spectral libraries are comprehensive collections representing optical properties of materials in a specific wavelength range. They are based on materials measured under standardized laboratory or field conditions including a geochemical validation of the material at hand. Spectral libraries are essential in the field of reflectance spectroscopy for example for mapping purposes. The results are hyperspectral images that serve for the detection and mapping of elemental or mineral occurrences in natural and in artificial surfaces. Examples for applications are large-area satellite or aerial surface mappings for geological exploration in early-stage field prospection. Future hyperspectral imaging satellites will provide the necessary data quality requirements to successfully map rare earth elements (REEs), copper deposits and other resources from space. These satellites will play a major role in the future of geological exploration, to help mapping large mineralized areas in remote regions (Mielke et al., 2016; Swayze et al., 2014). Several global mapping satellite missions will be launched in the next few years.. Amongst them are the German EnMAP, the Chinese CCRSS-A and the Japanese HISUI missions (Guanter et al., 2015; Iwasaki et al., 2011; Tong et al., 2014). For those missions, the imaging spectroscopy community is currently developing methodologies for e.g. the detection of REEs in the image spectra (Boesche et al., 2015; Boesche, 2015; Bösche, 2015; Herrmann, 2019; van der Meer et al., 2012; Turner et al., 2014a, 2014b; Turner, 2015). Hyperspectral data can also be acquired by ground- or UAV-based outcrop scans to study an orebody's surface geometry and mineral distribution (Figure 1) and can be applied in the laboratory on thin sections, samples, as well as drill cores to analyse and visualize melt evolution or zonation at a smaller scale.
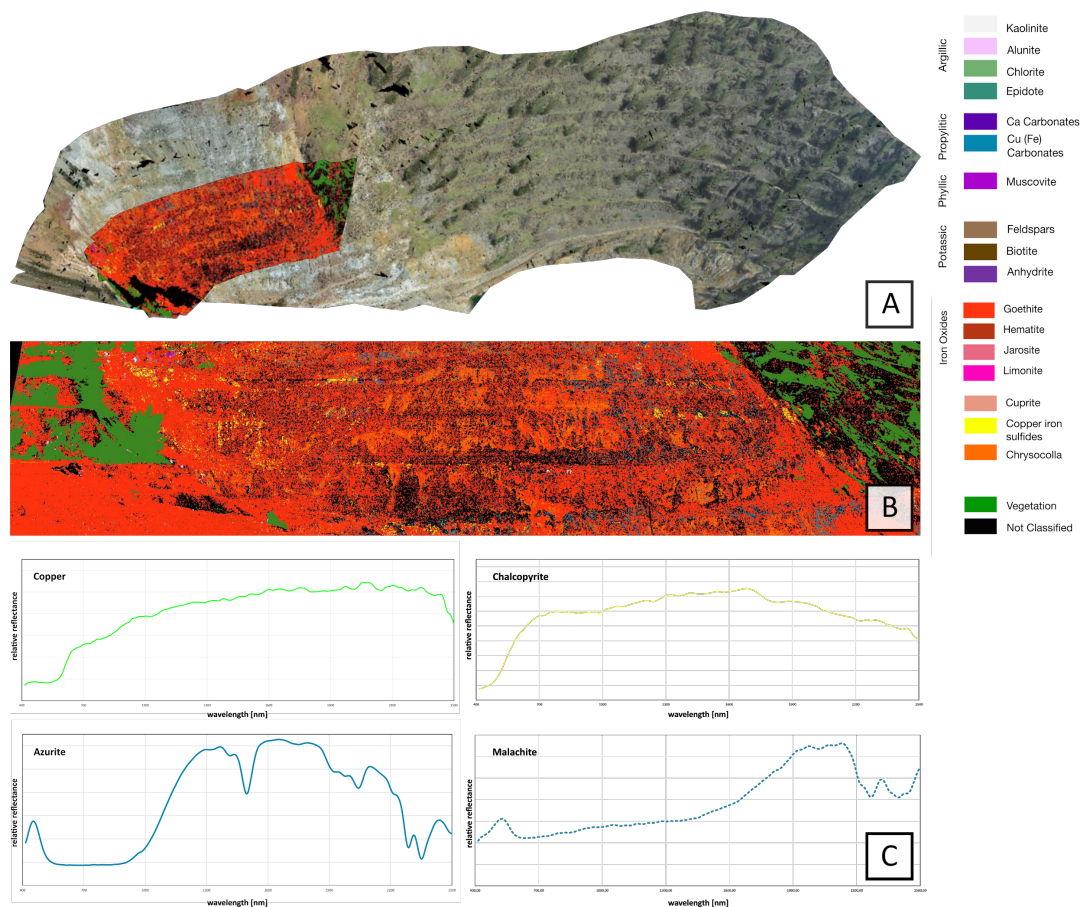
Figure 1: Example for the application of a spectral library. A) 3D modelling based on 79 RGB images and one RGB HySpex scene from the Apliki mine in the Republic of Cyprus. The mineral analysis from B) is stacked on the 3D model for visualisation purposes. B) Analysis based on HySpex scene analysed by EnGeoMap 2.0 using a custom-made spectral library from USGS spectra (Mielke et al., 2016). C) Example of hyperspectral spectra from copper bearing minerals as presented in Koellner et al. (2019).

The methods developed for the upcoming hyperspectral satellite missions like EnMap (Guanter et al., 2015) use image spectra as a database for their analysis. The image scenes are acquired by a moving line scanner mounted on the satellite, which records the spatial dimension (x- and y-dimension) line by line, as well as the wavelength dimension (z-dimension). Each pixel therefore represents the full spectral range of the sensor. The sensor's movement along a rotation or a movement

65 axis provides spatially continuous imaging spectroscopy data. Variations along the spectral domain of the data are visible as concave indentions, often referred to as "absorption bands". They are characteristic for the measured surface material and enable its identification and quantification (Clark, 2003). The recorded spectral information is a function of the chemical and physical properties of the target material and the sensor setup itself. Typical copper-bearing hyperspectral spectra are shown Figure 1C. We are presenting four spectral libraries and their geochemical validation. The libraries consist of the spectral

70 information of three different mineral groups: (1) powders of REE-bearing minerals and (2) REE-oxides (Koerting et al., 2019a), (3) copper-bearing minerals without any sample preparation (Koellner et al., 2019) and (4) powders of copper-bearing surface material from the Apliki copper-gold-pyrite mine in the Republic of Cyprus with the corresponding GPS position of the samples (Koerting et al., 2019b) . Spectrally, the libraries cover the full wavelength range of the solar optical range (400 nm – 2500 nm). We hereby contribute to the widely applied and accredited libraries, e.g. the USGS Spectral

75 Library (Hunt, 2002; Kokaly et al., 2017). The geochemical validation for each sample type is explained in methods. The two REE libraries (Koerting et al., 2019a) consist of the spectra of 16 rare earth oxides (REO) powders and 14 REE-bearing minerals (REMin). In addition, the spectra of niobium- and tantalum oxide are provided, which will further not be mentioned individually but be included in the term "REO". The third spectral library includes 20 different copper bearing minerals (Koellner et al., 2019b) and the fourth spectral library

80 contains 37 samples from the Apliki copper-gold-pyrite mine site in the Republic of Cyprus (Koerting et al., 2019b).
A list of all the samples can be found in the supplements.
The materials were spectroscopically examined using two spectrometers included in the HySpex system (VNIR-1600, SWIR-320m-e (technical description available at: https://www.hyspex.no/products/disc.php, 2019).
The outline of this study is based on the necessary knowledge to successfully make use of the here presented spectral

85 libraries. Chapter 2 includes a description of the analysed materials and Chapter 3 informs about the sample preparation and spectra collection. Chapter 4 describes the hyperspectral data acquisition, covering the processing of the data and spectral measurement parameters and Chapter 5 presents the geochemical analyses of the samples. Chapter 6 discusses the parameters influencing the data. The spectral libraries can be downloaded as an ASCII *.txt file format and as binary spectral library files format *.sli, and its associated header files *.hdr. An extensive data description and the geochemical

90 analysis results are included in the data publications , (Koellner et al. 2019; Koerting et al. 2019a; Koerting et al. 2019b).

95

2. Materials

The here presented spectral libraries comprises spectra of REEs (Koerting et al., 2019a), copper-bearing minerals (Koellner et al., 2019) and surface samples from the former copper-gold-pyrite mine Apliki in the Republic of Cyprus (Koerting et al., 2019b). The REE sample material comprises 16 REO powders (REO) and 14 REE bearing minerals (REMin). The used

100 REO powders belong to a series of rare earth metals and compounds (REacton®) and were received from Alfa Aesar. All REO powders contained at least 99.9% of the specified REE and were delivered together with concentration certificates, these geochemical certificates can be found in the data description of Koerting et al. (2019a). The REO powders were obtained as high-purity materials with a grainsize of <63 µm. The REMin samples (ore minerals) were purchased from Gunnar Färber Minerals, an online trader of mineral specimen. The mineral denotation is based on the sample name provided

105 by Gunnar Färber Minerals. The X-Ray Fluorescence (XRF) data presented in the data description of Koerting et al. (2019a) should be consulted to validate the given mineral denotations by Färber Minerals. A sample list for the REMin can be found in A2, for the REO in A3 of the appendix.

The copper bearing minerals belong to collections of the University of Potsdam (UP) and the Federal Institute for Geosciences and Natural Resources (BGR), a samples list can be found in the appendix (A4-A5). The minerals were

110 measured hyperspectrally with no sample preparation, the sample photos are provided in the data description for Koellner et al. (2019). The Apliki mine samples (Koellner et al., 2019) were collected in March 2018 during a measurement campaign of the Geological Survey Department of the Republic of Cyprus (GSD) and the GFZ German Research Centre for Geosciences (GFZ). Surface material in the mine was collected and prepared for geochemical analysis by Bureau Veritas Minerals (BVM). The powdered samples were measured hyperspectrally, a sample list including photos from the in-situ conditions of

115 the samples can be found in A6 of the appendix and in (Koerting et al., 2019b). An overview on sample types and their corresponding sample description in the appendix are listed in Table 1.

Table 1: Table of sample material and where to find the corresponding sample description tables.

Sample Material	Sample description in Supplements
REMin	S1
REO	S2
Copper bearing minerals	S3, S4
Apliki mine powders	S5

120

3. Sample Preparation and spectra collection

The sample preparation varied by sample type and depends on the material and the information of interest.

The spectra for each sample were manually extracted from the hyperspectral image scenes using an averaging of a number pixels and collected in a spectral library. Thereby each spectrum of a spectral library represents an average spectrum of the
125 material, depending on the sample size and spectrally homogeneity. The extraction of the spectra is explained in detail in each data description (Koellner et al. 2019; Koerting et al. 2019a; Koerting et al. 2019b).

For the REE samples, REMin and REOs, powders were measured in 100% quartz glass petri dishes underlain by black cellular rubber. For all measurements the final spectral analyses were spatially reduced to the center pixel of each sample
130 holder. Shadow effects from the sidewalls of the boxes could therefore be minimized. One representative spectrum of every sample was produced for the spectral library. In order to improve the signal-to-noise ratio and reduce the influence of outlier pixel, an average spectrum of sample-covering pixels was produced (Herrmann, 2019).

The copper mineral samples were measured with no sample preparation as the variable surface of the minerals and the
135 influence of the mineral structure was of interest. Figure 2 shows an exemplary scan of a part of the copper bearing minerals. Table A5 in the appendix shows the area for the geochemical sampling encircled in yellow. The same area was used to obtain the spectrum, averaging over a 5 by 5 pixel window.

140 **Figure 2: Showing HySpex scan "MH_FK_LAB_Cudetect_008_09012018_WR20" exemplary to highlight the non-existent sample preparation.**

145 The Apliki mine samples were crushed and powdered to ≥85% of the sample passing smaller than 75μm. Homogenized powders were measured as pressed powder tablets (Figure 3). The area to obtain the sample's spectra was chosen over a 5 by 5 pixel window, in the centre of the powder tablet to minimize influences from the tablets metal frame. The dark spots in each tablet were caused by previous measurements with a laser induced breakdown spectrometer (LIBS). The hyperspectral

sample spots were chosen in order to exclude the measurement points of the LIBS in the spectral footprint. In case of broken

150   powder tablets like "7d_Hem", the shadowed, rough surface areas were also excluded from the spectral sampling.
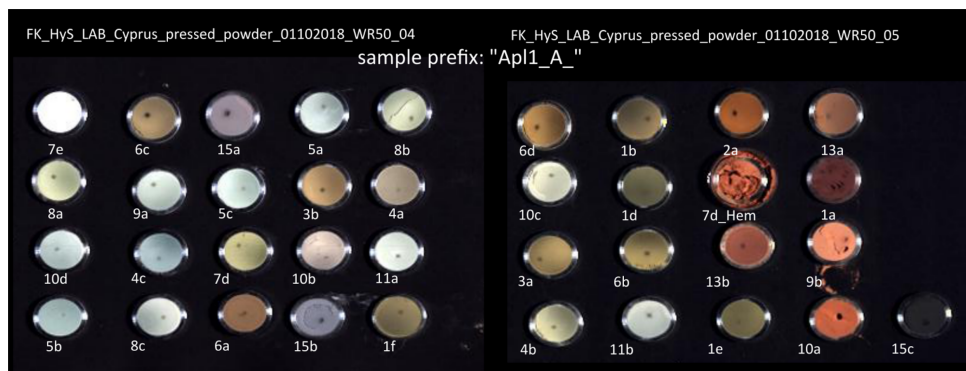
Figure 3: Showing the Apliki mine samples prepared as powder tablets.

155   **4. HySpex Data Recording**

The **HySpex VNIR-1600** and **SWIR-320m-e** (technical description available at: https://www.hyspex.no/products/disc.php, 2019) are two line-scanning cameras. The two cameras are mounted in parallel. They cover the range of the visible to near infra-red (VNIR, 400 – 1000 nm) and the short-wave infra-red (SWIR, 1000 – 2500 nm). They record an array-line of 1600 pixel (VNIR) and 320 pixel (SWIR) (push-broom scanning). Every pixel contains a spectrum with a total spectral sampling

160   number of 408 bands in total.

The HySpex cameras are provided with two acquisition modes, one for airborne data collection and one for laboratory measurements. In laboratory mode, the cameras are combined with a trigger pulse moving sleight (translation stage) of definable frame period (depending on the integration time of every array-line acquisition). The configuration of the translation stage framework, the cameras and the light source (45° illumination angle) are fixed, while the sleight and the

165   samples are moving through the focal plane (Rogass et al., 2017).

The reflectance level of a white reference panel, placed in line with the samples, is chosen according to the albedo of the samples. The higher the albedo of the sample, the higher is the diffuse reflectance factor of the white reference panel that is chosen. For the REE samples (REMin and REO), a white reference panel of 95% reflectance was used, because most of the samples were bright, white powders of a high albedo. The Apliki samples required a 50% reflectance white reference panel,

170   whereas the copper bearing minerals were measured using a 20% reflectance white reference panel. Both the geometrical setup and the heat up time of the lamp influence the configuration of the light source. The maximum illumination was obtained with a certain angle of 45° between incident light and the vertical plane. The distance between lamp and HySpex

cameras was higher compared to the distance between samples and sensor to ensure diffuse illumination and to avoid thermal influence on the cameras and the samples. The integration time (= measurement time for each image line) was tested

175   to be as high as possible to suppress the impact of signal uncorrelated gaussian white noise and at the same time as low as needed to avoid detector saturation. For all measurements the integration time was chosen with respect to the sample albedo. The used settings for the REMin and REOs are listed in Table 2, the settings for the copper bearing minerals in Table 3 and for the Apliki mine samples in Table 4 . The laboratory is equipped with black-painted walls and doors, as well as black curtains to avoid reflected light from surfaces other than the sample, an exemplary setup can be seen in Figure 4. The

180   laboratory conditions were kept stable, the air temperature was regulated to 21±0.5°C and the humidity was below 70% for all measurements. Black cellular rubber is used as a base material for all samples for hyperspectral data acquisition. It reflects less than 5 % on average of the incoming radiation.

Detailed descriptions for the GFZ' standard measurements and the process chain can be found in (Rogass et al., 2017).

185
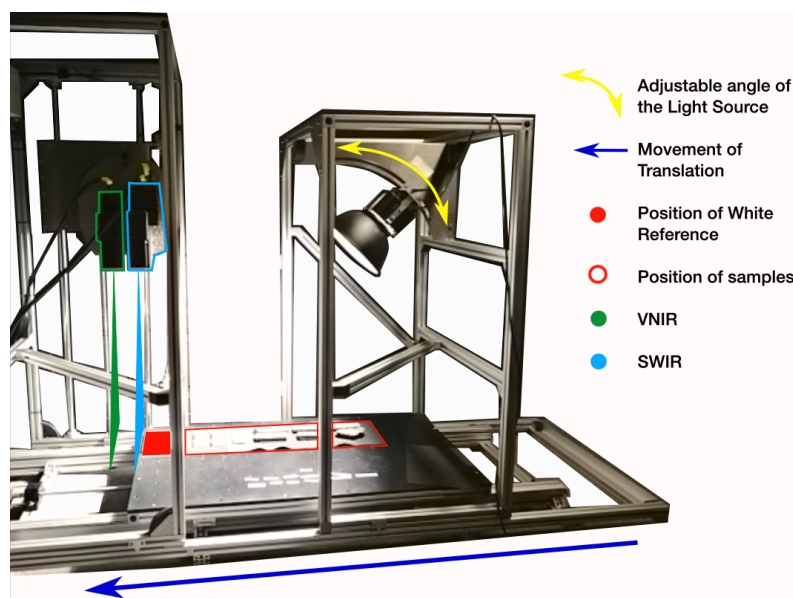
Figure 4: The HySpex translation stage setup (Körting, 2019)**.**

190 **Table 2: HySpex settings for laboratory measurements of the REO and REMin (Koerting et al., 2019a, modified after** (Boesche, 2015; Herrmann, 2019)**.**

HySpex settings		
Lamp arrangement	45°	
Distance, sample to sensor	1 m	
Sensor arrangement head to head	1m lenses, eq on VNIR	
Wavelength range	400 to 2500 nm	
	VNIR	SWIR
Sampling interval	3.7	6
Radiometric resolution	12 bit	14 bit
Light source	2 x 1000 W	
	VNIR (1600 px)	SWIR (320 px)
Frames	variable	variable
Integration time [µs]	30 000	5 000
Frame period [µs]	31 000	123 506

Table 3: HySpex settings for laboratory measurements of the copper bearing minerals, (Koellner et al., 2019)**.**

HySpex settings		
Lamp arrangement	45°	
Distance, sample to sensor	30cm	
Sensor arrangement head to head	30cm lenses, eq on VNIR	
Wavelength range	400 to 2500 nm	
	VNIR	SWIR
Sampling interval	3.7	6
Radiometric resolution	12 bit	14 bit
Light source	2 x 1000 W	
	VNIR (1600 px)	SWIR (320 px)
Frames	variable	variable
Integration time [µs]	120000 - 140000	15000 – 20000
Frame period [µs]	120062 - 141004	478334 - 561768

195

200 **Table 4: HySpex settings for laboratory measurements of Apliki mine powdered samples** (Koerting et al., 2019b) **.**

HySpex settings		
Lamp arrangement	45°	
Distance, sample to sensor	1 m	
Sensor arrangement head to head	1m lenses, eq on VNIR	
Wavelength range	400 to 2500 nm	
	VNIR	SWIR
Sampling interval	3.7	6
Radiometric resolution	12 bit	14 bit
Light source	2 x 1000 W	
	VNIR (1600 px)	SWIR (320 px)
Frames	variable	variable
Integration time [µs]	60000	10000
Frame period [µs]	60060	239282

205 **Hyperspectral Data Processing**

Each measurement run produces one VNIR and one SWIR 3D-data cube. The three dimensions are the two spatial x,y- and the spectral z-dimension. The 3D image cubes are produced, by moving a homogeneous reflecting white reference panel and the samples through the focal plane of the two sensors. These image cubes are then co-registered, resized and stacked to a continuous image cube. In order to produce a reflectance image, the image pixel that show the white standard were averaged

210 to a one-line reference spectrum. The reflectance was calculated by dividing every image line spectrum by its reference spectrum from the reflecting white reference panel. A detailed description for the laboratory set-up and processing can be found in (Rogass et al., 2017). The software 'HySpex ground' is used to perform the measurements and the software 'HySpex rad' is used to perform the radiometric calibration on the image data.

215 **5. Geochemical Sample Analysis for Validation**

Depending on the sample type, the geochemical validation methods differ. The methods used for each sample type, can be found in Table 5.

220

Table 5: Sample type and corresponding geochemical validation method.

Sample type	Concentration level determination
REO (Koerting at al., 2019a))	Laboratory certificates
REMin (Koerting at al., 2019a)	X-Ray Fluorescence (XRF), Electron microprobe analyser (EMPA) analyses
Copper bearing minerals (Koellner at al., 2019)	Scanning electron microscope (SEM), EMPA analyses
Apliki mine samples (Koerting at al., 2019b)	Bureau Veritas Minerals Analysis

5.1 Thermo Niton XL3t (XRF)

225 The geochemical validation measurements for the REMins were performed using an X-Ray Fluorescence (XRF) instrument - Thermo Niton XL3t (Fisher Scientific, 2002).

The XL3t is a light-weight, mobile XRF analyzer. The measurement principle follows the principle of X-Ray fluorescence, where the sample inbound X-Rays excite electrons to a higher energy level in the sample material. Energy in form of XRF radiation is released when these electrons return to their original state. The frequency of this radiation is characteristic for the

230 measured chemical element and its intensity is correlated to the concentration level. The intensity of each element is detected as counts per second by the detector, a geometrically optimized large area drift detector (GOLDD). The maximum excitation voltage of the XL3t device is 50 kV, which means out of the full REE suite only four light REEs can be detected (Lanthanum, Cerium, Neodymium and Praseodymium).

The XL3t spectrometer is attached to a lead shielded sample chamber, in which samples with a diameter smaller than 3.3 cm

235 can be placed. Mineral samples can be directly placed in the chamber; powdered samples have to be placed in sample tubes (2.5 cm diameter). The sample tubes are made of a plastic tube with a plastic foil on the bottom. The plastic cannot be detected by XRF and therefore not interfere with the measurements. A build-in camera of the XL3t enables the precise location of the measuring spot. The used software for the measurements is named "NDTr" and the measurement mode was the "mining and exploration" mode. The concentration levels are provided along with a balance value. "Balance" represents

240 counts per seconds that could not be identified to one of the measured elements. Table 6 shows the measurement modes and filters used. In-depth description of the XL3t and the XL3t-results for each sample can be found in (Herrmann, 2019).

245 **Table 6: Settings used for the Thermo Niton XL3t X-ray fluorescence device.**

Thermo Niton XL3t Setting	
Measurement mode	Test all geo
Filter	Main, Low, High, Light
Filter measurement time	30 seconds each

5.2 Scanning Electron Microscope (SEM) and Electron Microprobe Analyzer (EMPA)

Some of the REEMin (xenotime, bastnaesite, fluorapatite, synchisite and ilmenite) were additionally analysed by using a

250 JEOL JXA-8200 electron microprobe (EMPA) at the University of Potsdam. The conditions used for the analysis were: 20kV acceleration voltage, 20nA beam current and a beam size of 2 μm. Counting times were between 10 s - 20 s on peak for major elements and 50 s for REE and other trace elements, respectively. The following spectral lines and mineral standards from Smithsonian and Astimex were used: fluorapatite (F Kα, P Kα, Ca Kα), albite (Na Kα), fayalite (Fe Kα, Mn Kα), wollastonite (Si Kα), omphacite (Al Kα), $LaPO_4$ (La Lα), $PrPO_4$ (Pr Lβ), $CePO_4$ (Ce Lα), $NdPO_4$ (Nd Lβ), YPO_4 (Y

255 Lα), $EuPO_4$ (Eu Lα), $SmPO_4$ (Sm Lβ), $LuPO_4$ (Lu Lα), $GdPO_4$ (Gd Lα), $ErPO_4$ (Er Lβ), $DyPO_4$ (Dy Lβ), $YbPO_4$ (Yb Lα), $HoPO_4$ (Ho Lβ), monazite (Th Mα, U Mβ, Tb Lα), uranothorite (U Mβ), crocoite (Pb Mβ). The EMPA data were reduced using the PRZ-XXP correction routine.

In order to obtain information about the chemical composition, zonation and internal fabrics of the copper samples a fully

260 automated JEOL JSM-6510 scanning electron microscope (SEM) (20kV acceleration voltage) at the University of Potsdam, was used. A back-scattered electron detector displays compositional variation of light and heavy elements across the imaging area.

An energy dispersive X-ray spectrometer (EDX, Oxford Instruments INCAx-act) attached to the instrumentation provides quantitative elemental analysis of single spots. After calibrating with pure copper, a wide spectrum of elements can be

265 qualified. According to experience, divergences of up to 5 weight % can be expected, which for the quantitative analysis can be neglected. The software interpolates the weight % of the detected elements of a total to 100 weight %.

In order to approximate the values for copper a JEOL JXA-8200 electron microprobe (EMPA) at the University of Potsdam was used. The electron microprobe is equipped with five wavelength-dispersive X-ray spectrometers (WDX) and was

270 operated with a 20 kV accelerating voltage, a 20 nA current, and a beam diameter of 2 μm. The analytical counting times were 20/10 s for the element peak and 10/5 s for background positions. Analyses were standardized against natural silicates/sulphides obtained from the Smithsonian Institution and Astimex. Quantifying elements of a lower atomic mass than boron is not possible, carbon cannot be measured either. The EMPA measurements are therefore limited by the fact that the carbon and water content cannot be validated.

275

An example analysis for copper mineral sample K1 can be seen in Figure 5 and Table7, the full EMPA and SEM data files are documented in (Koellner et al., 2019) http://doi.org/10.5880/GFZ.1.4.2019.003.
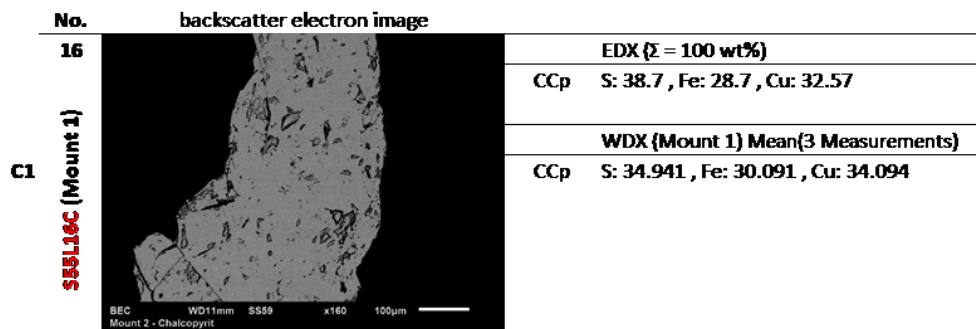
280

Figure 5: Sample C1 SEM and EMPA analysis example

Tab. 7: Sample C1 EMPA analysis example, 3 measurement spots for each sample (S55L16c-1 – 3 in the "comment"). Element

285 concentrations reported as wt%.

Sample	Al	Hg	Fe	Cu	Si	S	Mn	Total	Comment
C1	-	0.035	30.002	33.98	-	34.805	0.002	98.824	S55L16c-1
C1	-	0	30.193	34.108	0.003	34.931	0.004	99.239	S55L16c-2
C1	-	0.001	30.077	34.194	-	35.086	-	99.358	S55L16c-3

5.3 Apliki mine sample analysis at Bureau Veritas Minerals

The Apliki mine samples were analysed by Bureau Veritas Minerals (BVM). The analysis was split in groups based on the

290 analysis type, in this case "aquatic", "rock" and "soil". The sample numbers, analysis type and BVM analysis codes can be found in Table 8, an explanation of the BVM codes is provided in Table 9. One sample was analysed with the Aquatic analysis type, the Rock analysis type included 25 samples and Soil analysis type included eleven samples.

295

Table 8: Apliki mine samples and the corresponding analysis type and BVM code (See Table XX / Appendix for sample description)

Analysis type	Samples with prefix "AP/1-A"-	BVM code
Aquatic	1a	SHP01, CRU80, PULHP, AQ250
Rock	1b, 1d, 1e, 4c, 5a, 5b, 5c, 7d, 7d-Hem, 7e, 8a, 8b, 8c, 9a, 9b, 10a, 10b, 10c, 10d, 11a, 11b, 13a, 15a, 15b, 15c	SHP01, PRP70-250, TC000
Soil	1f, 2a, 3a, 3b, 4a, 4b, 6a, 6b, 6c, 6d, 13b	SHP01, PRP70-250, DISP2, TC000

300

Table 9: Sample preparation and description of the BVM according to their sample type

BVM Code	Description
SHP01	Per sample shipping charges for branch shipments
CRU80	Crush to 80% passing 10 mesh
PULHP	Hand Pulverize samples mortor and pestle
AQ250	Ultra Trace Geochemical Aqua Regia digestion, 1:1:1 Aqua Regia digestion (HNO3-HCl acid digestion), Ultratrace ICP-MS analysis
PRP70-250	Crush, split and pulverize 250 g rock to 200 mesh
LF302-EXT	Lithogeochemical Whole Rock Fusion, LiBO2/LiB4O7 fusion ICP-ES analysis Comment: Major oxides do not sum to 100% due to possible incomplete fusion of some minerals or other element oxides may be present.
DISP2	Heat treatment of Soils and Sediments.
TC000	Carbon and Sulphur Analysis

6. Validation and Discussion

305

This section will discuss the technical validation of the results in terms of sample material properties, systematic errors and variation of measurements (experimental error).

Sample Material Properties

310 The REO powders were certified to contain at least 99.9% of the corresponding REO. The certificates are listed in (Koerting et al., 2019a). The REE mineral samples were geochemically analysed using the Thermo Niton XL3t (Fisher Scientific, 2002) device. The resulting element concentrations and the measurement error (2σ) are provided in Koerting et al. (2019a). The validation for the Copper bearing minerals can be found in Koellner et al. (2019) and the Apliki mine sample validation, analysed by BVM, can be found in Koerting et al. (2019b).

315

Systematic Errors of hyperspectral data acquisition

Systematic errors are discussed based on instrument drift, calibration and optimization of measurements. Initializing a warm-up phase of optical components, detectors and lamps, reduced influences due to instrument drift. Additionally, laboratory conditions were monitored to ensure a stable temperature and humidity. The HySpex cameras and the reference standards are

320 factory calibrated once per year. Measurements used for the final spectral library were collected within one calibration time span to ensure equal acquisition conditions. For HySpex, an average of multiple measurements minimized measurements variations. An average (median) of 500 to 800 pixel spectra was taken for the HySpex REE and REO spectra. This number relates to the maximum number of non-disturbed pixels per sample region of interest (e.g., pixels that were not shadowed from the sample holder side walls, etc.). For the copper bearing minerals and the Apliki mine powders a 5x5 average pixel

325 window was chosen over the area of interest. For these samples using a smaller pixel number for the average was necessary as the sampling of the copper-bearing minerals for geochemical validation occurred over a small area of the sample and the Apliki mine powder tablets were too small to ensure a bigger homogenous area.

Measurements variation

330 Variations of measurements were not only based on instrument calibrations or drift. They can also occur due to the detector geometry or geochemical properties of the minerals. These variations may appear as a shift of the peak positions of the absorption bands. This means, different hyperspectral sensors will show variations in the spectrum of the same material. By only using one set of hyperspectral sensors, the HySpex VNIR and SWIR, these shifts will not appear in our data sets. They might show when comparing our spectra of a material with spectra taken from a different instrument. Mineral spectra also

335 differ when comparing different minerals of the same mineral denotations e.g. "Malachite" to each other. The spectral signal

differs for example due to changes in geochemistry, physical appearance e.g. crystallization and weathering grade (Misra et al., 1992). This is why we included the geochemical validation data in the available data.

XL3t systematic errors

340 The XL3t is internally calibrated and provides an internal warm-up phase to guarantee stable measurement conditions. Unlike the spectrometer measurements, experimental error was only provided for the XL3t. In order to reduce the experimental error, the measurement time was set to 120 seconds. The XL3t collects the emitted radiation from the sample using four different filters. While the sample was irradiated, each filter measures counts per second within a time span of 30 seconds. Next, the average counts per second were internally transformed to ppm. The irradiation of, in total, 120 seconds

345 per sample was empirically tested to enable short measurement duration in combination with the lowest achievable standard deviation of concentration level.

7. Data Availability

The here described spectral libraries are published under the Creative Commons Attribution International 4.0

350 **Licence (CC BY 4.0) via GFZ Data Services. Due to the different types of samples, we are presenting the following three data publications: (1) 32 rare-earth minerals and rare-earth oxides including niobium- and tantalum-oxide (Koerting et al., 2019a, http://doi.org/10.5880/GFZ.1.4.2019.004); (2) Mineral spectra and chemistry of 20 copper bearing minerals (Koellner et al., 2019; http://doi.org/10.5880/GFZ.1.4.2019.003) and (3) Mineral spectra and chemistry of 37 copper bearing surface samples from Apliki copper-gold-pyrite mine in the Republic of Cyprus**

355 **(Koerting et al., 2019b; http://doi.org/10.5880/GFZ.1.4.2019.005).**

8. Sample Availability

The samples provided by the BGR are available through the collection of the BGR Spandau by their sample name in table A5 in the supplements (https://www.gewis.bgr.de). The samples provided by the GFZ and UP belong to projects and have to be requested separately.

360

365 **9. Appendices**

Tab A1: List of not commonly known terms used throughout the paper (acronyms)

Terms	Abbreviation	Description
Abbreviation	REE	Rare Earth Element
	REO	Rare Earth Oxide
	REMin	Rare Earth Element bearing Mineral
	VNIR	Visible light and near infrared
	SWIR	Short wave infrared
	XRF	X-Ray fluorescence
	EnMAP	Environmental Mapping and Analysis Program: future earth observation satellite mission (www.enmap.org)[1]
	CCRSS-A	China Commercial Remote Sensing Satellite System: future earth observation satellite mission
	HISUI	Hyperspectral Imager Suite: future earth observation satellite mission
Instruments	HySpex VNIR-1600	HySpex pushbroom spectrometer, VNIR camera
	HySpex SWIR-320m-e	HySpex pushbroom spectrometer, SWIR camera
	HySpex ground	HySpex operational software for laboratory and near-field application
	HySpex rad	HySpex calibration software to transform raw DN into radiance data
	Thermo Scientific Niton XL3t	Thermo Scientific Inc. X-Ray fluorescence analyzer (NITON TM XL3t)
	NDTr	Thermo Scientific Inc. NITON TM operational software
	JEOL JXA-8200	Electron microprobe analyser (EMPA)
	JEOL JSM-6510	Scanning electron miscroscope (SEM)

	Oxford Instruments INCAx-act	Energy dispersive X-ray spectrometer (EDS)
Registered brands, copyrights and/ or other protected terms	REacton®	Series of rare earth metals and compounds
	Alfa Aesar	Manufacturer and supplier of chemicals for research and development (today: Thermo Scientific Inc.)
	Gunnar Färber Minerals	Supplier of mineral specimen
	REEMAP	Rare Earth Element MAPping: Research project for the development of a modular multi-sensor processing chain for modern imaging spectrometers to detect REEs
	Smithonian Institution	Smithsonian Institution Department of Mineral Sciences, reference material from the Smithonian Microbeam Standards
	Astimex Standards Ltd.	Astimex produces standards suitable for electron microprobe and scanning electron miscroscop X-ray analysis.
	BVM	Bureau Veritas Minerals is an industry leader in the analysis of minerals for the Exploration and Mining industries. BVM is a service company that provides mineral preparation and laboratory testing services.
Research and federal institutes	BGR	Federal Institute for Geosciences and Natural Resources
	GSD	Geological Survey Department of the Republic of Cyprus
	UP	University of Potsdam
	GFZ	German Research Centre for Geosciences

10. Author contributions

370 *Apliki mine and copper bearing minerals:* Friederike Koerting designed the Apliki sample related study, performed and supervised the measurements for Marcel Hornings data and the Apliki samples and wrote the manuscript. Nicole Koellner designed the copper sample study, supervised the measurements and performed the geochemical analysis at the University of Potsdam. Marcel Horning performed most of the measurements on the copper samples and prepared the spectral copper library. Pia Brinkman prepared the Apliki sample powder tablets. Christian Mielke, Agnieszka Kuras, Constantin Hildebrand

375   and Friederike Klos prepared parts of the spectral libraries. *REE minerals and REOs:* Nina K. Boesche designed the REE study, performed some measurements, and supervised the REE measurements. Sabrina Herrmann prepared the samples and conducted most of the measurements. Christian Rogass developed and applied the HySpex post-processing chain. Christian Mielke and Kirsten Elger helped revising the manuscript. Uwe Altenberger supervised the studies and gave some valuable comments on the manuscript.

380

11. Competing interests
The authors declare no conflict of interest

12. Acknowledgements
385   We would like to thank the Helmholtz Centre Potsdam GFZ German Research Centre for Geosciences for providing the infrastructure and personnel support to conduct our research. Our gratitude also goes to the German Federal Ministry of Education and Research and the r4 subsidy program for innovative technologies for resource efficiency, which supported the REEMAP scientific project. We also thank the DLR Space Administration and the German Federal Ministry for Economic Affairs and Energy for the financial support based on a decision by the German Bundestag in the frame of the EnMAP
390   scientific preparation program (Contract No. 50EE1256). We also want to express our gratitude to Seltenerdmetalle24, in person Manuel Schultz, for his friendly service when providing laboratory standards and negative control sample holder. Thanks to the support by the GSD we were able to conduct a study and sample in the Republic of Cyprus and our thanks goes to our colleagues there for their help and directions in the unknown terrain.

395

400

405

13. References

Boesche, N., Rogass, C., Lubitz, C., Brell, M., Herrmann, S., Mielke, C., Tonn, S., Appelt, O., Altenberger, U. and Kaufmann, H.: Hyperspectral REE (Rare Earth Element) Mapping of Outcrops—Applications for Neodymium Detection,

410   Remote Sens., 7(5), 5160–5186, https://doi.org/10.3390/rs70505160, 2015.

Boesche, N. K.: Hyperspectral Rare Earth Element Mapping of Three Outcrops at the Fen Complex, Norway: Calcitic, Dolomitic, and Ankeritic Carbonatites, in Rare Earths Industry - Technological, Economic, and Environmental Implications, edited by I. B. De Lima and W. L. Filho, p. 434, Elsevier Inc. [online] Available from: https://www.elsevier.com/books/rare-

415   earths-industry/borges-de-lima/978-0-12-802328-0, 2015.

Bösche, N. K.: Detection of Rare Earth Elements and Rare Earth Oxides with Hyperspectral Spectroscopy, University of Potsdam. [online] Available from: http://nbn-resolving.de/urn:nbn:de:kobv:517-opus4-85363, , Dissertation University Potsdam.. 2015.

420

Clark, R. N.: Imaging spectroscopy: Earth and planetary remote sensing with the USGS Tetracorder and expert systems, J. Geophys. Res., 108(E12), 5131, https://doi.org/10.1029/2002JE001847, 2003.

Fisher Scientific: Thermo Scientific NITON ® XL3t NITON XL3t Specifications, Analysis [online] Available from:

425   https://www.thermofisher.com/content/dam/LifeTech/Documents/PDFs/china/Niton-XL3t-GOLDD-Spec-Sheet-
2013Jan15.pdf,, last access: 18 June 2019.

Guanter, L., Kaufmann, H., Segl, K., Foerster, S., Rogass, C., Chabrillat, S., Kuester, T., Hollstein, A., Rossner, G., Chlebek, C., Straif, C., Fischer, S., Schrader, S., Storch, T., Heiden, U., Mueller, A., Bachmann, M., Mühle, H., Müller, R.,

430   Habermeyer, M., Ohndorf, A., Hill, J., Buddenbaum, H., Hostert, P., Van Der Linden, S., Leitão, P. J., Rabe, A., Doerffer, R., Krasemann, H., Xi, H., Mauser, W., Hank, T., Locherer, M., Rast, M., Staenz, K. and Sang, B.: The EnMAP spaceborne

imaging spectroscopy mission for earth observation, Remote Sens., https://doi.org/10.3390/rs70708830, 2015.

Herrmann, S.: Capacity of imaging spectroscopy for the characterisation of REO, REE bearing minerals and primary REE-

435   deposits, Scientific Technical Report - Data ; 19/08, http://doi.org/10.2312/GFZ.B103-19089, 2019.

Norsk   Elektro   Optikk   AS   HySpex   VNIR1600   and   SWIR320   m-e:,   [online]   Available   from:

https://www.hyspex.no/products/disc/vnir-1600.php, last access: 18 June 2019

440   Hunt, G. R.: SPECTRAL SIGNATURES OF PARTICULATE MINERALS IN THE VISIBLE AND NEAR INFRARED,

GEOPHYSICS, https://doi.org/10.1190/1.1440721, 2002.

Iwasaki, A., Ohgi, N., Tanii, J., Kawashima, T. and Inada, H.: Hyperspectral Imager Suite (HISUI)-Japanese hyper-multi

spectral   radiometer,   in   International   Geoscience   and   Remote   Sensing   Symposium

445   (IGARSS).,http://doi.org/10.1109/IGARSS.2011.6049308, 2011.

Koellner, N., Koerting, F., Horning, M., Mielke, C. and Altenberger, U.: Mineral spectra and chemistry of 20 copper bearing

minerals., https://doi.org/ http://doi.org/10.5880/GFZ.1.4.2019.003, 2019

450   Koerting, F., Herrmann, S., Boesche, N. K., Mielke, C., Koellner, N. and Altenberger, U.: Mineral spectra and chemistry of

32 rare-earth minerals and rare-earth oxides including., http://doi.org/ http://doi.org/10.5880/GFZ.1.4.2019.004, 2019a.

Koerting, F., Rogass, C., Koellner, N., Horning, M. and Altenberger, U.: Mineral spectra and chemistry of 37 copper bearing

surface   samples   from   Apliki   copper-gold-pyrite   mine   in   the   Republic   of   Cyprus.,   https://doi.org/

455   http://doi.org/10.5880/GFZ.1.4.2019.005, 2019b.

Kokaly, R. F., Clark, R. N., Swayze, G. A., Livo, K. E., Hoefen, T. M., Pearson, N. C., Wise, R. A., Benzel, W. M., Lowers, H. A., Driscoll, R. L. and Klein, A. J.: USGS Spectral Library Version 7, Data Series, https://doi.org/10.3133/ds1035, 2017.

460 Körting, F.: Development of a 360 ° hyperspectral drill core scanner Test of technical conditions and validation of high-resolution near- field analysis of crystalline basement rocks using COSC-1 core samples., https://doi.org/ http://doi.org/10.2312/GFZ.b103-19071, 2019.

van der Meer, F. D., van der Werff, H. M. A., van Ruitenbeek, F. J. A., Hecker, C. A., Bakker, W. H., Noomen, M. F., van
465 der Meijde, M., Carranza, E. J. M., de Smeth, J. B. and Woldai, T.: Multi- and hyperspectral geologic remote sensing: A review, Int. J. Appl. Earth Obs. Geoinf., https://doi.org/10.1016/j.jag.2011.08.002, 2012.

Mielke, C., Rogass, C., Boesche, N., Segl, K. and Altenberger, U.: EnGeoMAP 2.0—Automated Hyperspectral Mineral Identification for the German EnMAP Space Mission, Remote Sens., 8(2), 127, https://doi.org/10.3390/rs8020127, 2016.

470

Misra, S. N., Mehta, S. B., Balar, B. M. and John, K.: Absorption difference and comparative absorption spectrophotometry of neodymium(iii) haloacetates in non-aqueous media and in crystalline state, Synth. React. Inorg. Met. Chem., https://doi.org/10.1080/15533179208020242, 1992.

475 Rogass, C., Koerting, F. M., Mielke, C., Brell, M., Boesche, N. K., Bade, M. and Hohmann, C.: Translational imaging spectroscopy for proximal sensing, Sensors (Switzerland), https://doi.org/10.3390/s17081857, 2017.

Swayze, G. A., Clark, R. N., Goetz, A. F. H., Livo, K. E., Breit, G. N., Kruse, F. A., Sutley, S. J., Snee, L. W., Lowers, H. A., Post, J. L., Stoffregen, R. E. and Ashley, R. P.: Mapping advanced argillic alteration at Cuprite, Nevada, using imaging
480 spectroscopy, Econ. Geol., 109(5), 1179–1221, https://doi.org/10.2113/econgeo.109.5.1179, 2014.

Tong, Q., Xue, Y. and Zhang, L.: Progress in hyperspectral remote sensing science and technology in China over the past three decades, IEEE J. Sel. Top. Appl. Earth Obs. Remote Sens., https://doi.org/10.1109/JSTARS.2013.2267204, 2014.

Turner, D., Rivard, B. and Groat, L.: Rare earth element ore grade estimation of mineralized drill core from hyperspectral

485   imaging spectroscopy, in International Geoscience and Remote Sensing Symposium (IGARSS)., https://doi.org/10.1109/IGARSS.2014.6947520, 2014a

Turner, D. J.: Reflectance spectroscopy and imaging spectroscopy of rare earth element-bearing mineral and rock samples., 2015, Dissertation, The University of British Columbia, Vancouver. April 2015. URL:

490   https://open.library.ubc.ca/cIRcle/collections/ubctheses/24/items/1.0167182. last access: 5 November 2019.

Turner, D. J., Rivard, B. and Groat, L. A.: Visible and short-wave infrared reflectance spectroscopy of REE fluorocarbonates, Am. Mineral., https://doi.org/10.2138/am.2014.4674, 2014b.

495